

# High-throughput quantitation of human neutrophil recruitment and functional responses in an air-blood barrier array

Cite as: APL Bioeng. 9, 026110 (2025); doi: 10.1063/5.0220367

Submitted: 24 May 2024 · Accepted: 19 November 2024 ·

Published Online: 25 April 2025






















View Online



Export Citation



CrossMark

Hannah Viola,<sup>1,2,3,a)</sup>  Liang-Hsin Chen,<sup>3</sup>  Seongbin Jo,<sup>2</sup>  Kendra Washington,<sup>3</sup>  Cauviya Selva,<sup>3</sup>  Andrea Li,<sup>3</sup>  Daniel Feng,<sup>3</sup>  Vincent Giacalone,<sup>4,5</sup>  Susan T. Stephenson,<sup>4,5</sup>  Kirsten Cottrill,<sup>4,5</sup>  Ahmad Mohammad,<sup>4,5</sup>  Evelyn Williams,<sup>3</sup>  Xianggui Qu,<sup>6</sup>  Wilbur Lam,<sup>3,7</sup>  Nga L. Ng,<sup>2,8,9</sup>  Anne Fitzpatrick,<sup>4,5</sup>  Jocelyn Grunwell,<sup>10</sup>  Rabindra Tirouvanziam,<sup>4,5,b)</sup>  and Shuichi Takayama<sup>1,3,b)</sup> 

## AFFILIATIONS

<sup>1</sup>Parker H. Petit Institute for Bioengineering and Bioscience, Georgia Institute of Technology, Atlanta, Georgia 30332, USA

<sup>2</sup>School of Chemical and Biomolecular Engineering, Georgia Institute of Technology, Atlanta, Georgia 30332, USA

<sup>3</sup>Wallace H. Coulter Department of Biomedical Engineering, Georgia Institute of Technology, Atlanta, Georgia 30332, USA

<sup>4</sup>Center for CF & Airways Disease Research, Children's Healthcare of Atlanta, Atlanta, Georgia 30322, USA

<sup>5</sup>Department of Pediatrics, Division of Pulmonology, Asthma, Cystic Fibrosis and Sleep, Emory University School of Medicine, Atlanta, Georgia 30322, USA

<sup>6</sup>Department of Mathematics and Statistics, Oakland University, Rochester, Michigan 48309, USA

<sup>7</sup>Aflac Cancer and Blood Disorders Center, Children's Healthcare of Atlanta and the Emory University School of Medicine, Atlanta, Georgia 30322, USA

<sup>8</sup>School of Earth and Atmospheric Sciences, Georgia Institute of Technology, Atlanta, Georgia 30332, USA

<sup>9</sup>School of Civil and Environmental Engineering, Georgia Institute of Technology, Atlanta, Georgia 30332, USA

<sup>10</sup>Department of Pediatrics, Division of Critical Care Medicine, Emory University School of Medicine and Children's Healthcare of Atlanta at Arthur M. Blank Hospital, Atlanta, Georgia 30322, USA

<sup>a)</sup>Present address: Biomedical Engineering and Biointerfaces Institute, University of Michigan, Ann Arbor, MI, USA.

<sup>b)</sup>Authors to whom correspondence should be addressed: [tirouvanziam@emory.edu](mailto:tirouvanziam@emory.edu) and [takayama@gatech.edu](mailto:takayama@gatech.edu)

## ABSTRACT

Dysregulated neutrophil recruitment drives many pulmonary diseases, but most preclinical screening methods are unsuited to evaluate pulmonary neutrophilia, limiting progress toward therapeutics. Namely, high-throughput therapeutic assays typically exclude critical neutrophilic pathophysiology, including blood-to-lung recruitment, dysfunctional activation, and resulting impacts on the air-blood barrier. To meet the conflicting demands of physiological complexity and high throughput, we developed an assay of 96-well leukocyte recruitment in an air-blood barrier array (L-ABBA-96) that enables *in vivo*-like neutrophil recruitment compatible with downstream phenotyping by automated flow cytometry. We modeled acute respiratory distress syndrome (ARDS) with neutrophil recruitment to 20 ng/mL epithelial-side interleukin 8 and found a dose-dependent reduction in recruitment with physiologic doses of baricitinib, a JAK1/2 inhibitor recently Food and Drug Administration-approved for severe Coronavirus Disease 2019 ARDS. Additionally, neutrophil recruitment to patient-derived cystic fibrosis sputum supernatant induced disease-mimetic recruitment and activation of healthy donor neutrophils and upregulated endothelial e-selectin. Compared to 24-well assays, the L-ABBA-96 reduces required patient sample volumes by 25 times per well and quadruples throughput per plate. Compared to microfluidic assays, the L-ABBA-96 recruits two orders of magnitude more neutrophils per well, enabling downstream flow cytometry and other standard biochemical assays. This novel pairing of high-throughput *in vitro* modeling of organ-level lung function with parallel high-throughput leukocyte phenotyping substantially advances opportunities for pathophysiological studies, personalized medicine, and drug testing applications.

© 2024 Author(s). All article content, except where otherwise noted, is licensed under a Creative Commons Attribution-NonCommercial-NoDerivs 4.0 International (CC BY-NC-ND) license (<https://creativecommons.org/licenses/by-nc-nd/4.0/>). <https://doi.org/10.1063/5.0220367>

## INTRODUCTION

Modulating neutrophilic inflammation has historically been challenging in respiratory medicine<sup>1,2</sup> despite an expanding pool of immunomodulators available for clinical use.<sup>3–6</sup> A major bottleneck has been the lack of preclinical screening tools that adequately capture human-specific neutrophil responses such as priming, while in the circulation, pathological recruitment into tissues, and the secondary acquisition of dysfunctional states therein.<sup>2,7–9</sup> Although animal models can capture complex tissue-level pathophysiology such as immune cell recruitment and activation,<sup>10,11</sup> their use is hindered by low throughput and, most importantly, evolutionary divergence between species. Rodents, for example, lack interleukin-8 (IL-8), a central neutrophil chemoattractant in human disease.<sup>10,12,13</sup> As an alternative, *in vitro* platforms have been developed to support human neutrophil-targeted drug screening.<sup>14–18</sup> So far, however, technical demands and practical constraints of *in vitro* systems for human neutrophil-focused drug screening have limited their impact. Since candidate therapies aim to influence functional behavior of neutrophils, such as their recruitment, priming, activation, and signaling to resident tissue cells, these must be featured in screening models.<sup>2</sup> Consequently, transmigration systems are needed that incorporate disease-relevant stimuli and allow neutrophil engagement with both endothelium and epithelium to induce their physiological cascade of activation.<sup>19,20</sup> Such advanced transmigration models must be coupled to a practical downstream workflow that reduces cost and uses accessible technologies to deliver relevant, functional outcomes with high throughput.<sup>21,22</sup>

Microphysiological systems (MPSs) use human cells in co-culture to capture emergent functional behaviors of multicellular systems, like immune cell recruitment, paracrine signaling loops, and mucosal barrier function.<sup>23,24</sup> MPS must balance throughput, robustness, physiologic relevance, efficient use of limited human cells and clinical samples, and the provision of quantitative assay outcomes.<sup>21,24</sup> Microfluidic “lung-on-a-chip” devices are prominent lung MPSs that often feature bilayer epithelial-endothelial co-culture to mimic the alveocapillary (i.e., air-blood) barrier. Microfluidics can also apply physiologic forces like shear, strain, and compression to the air-blood barrier to modulate its properties.<sup>24–27</sup> However, trans-endothelial/epithelial immune cell recruitment assays in microfluidics are constrained. Microfluidics’ small size precludes recruitment of more than 10s–100s of neutrophils per chip,<sup>16,28–30</sup> an insufficient amount for downstream phenotyping with reliable, established methods like flow cytometry. Performing non-terminal barrier measurements in microfluidics, such as trans-epithelial electrical resistance (TEER), requires custom device engineering.<sup>31</sup> Mechanical stress imparted microfluidic channels during neutrophil retrieval could affect their phenotype, skewing outcomes.<sup>32,33</sup> Finally, generating and culturing microfluidic lungs-on-a-chip typically requires bespoke equipment and advanced technical skills that are inaccessible outside of specialized laboratories, limiting their overall reach.<sup>34</sup> Under these limitations, the few microfluidic transmigration models reported have only measured the number of migrated cells and/or their rolling velocity, both using representative images from low-throughput microscopy.<sup>16,28–30,35,36</sup>

The Boyden chamber is a second well-known platform consisting of a porous plastic membrane that separates a culture well so that cells migrate from the top to bottom chamber. Typical assays, like Transwell<sup>®</sup> and Alvetex<sup>®</sup> filters in 12- to 24-well plate format, can recruit adequate neutrophils from the top to bottom chamber for downstream

immunophenotyping.<sup>37–39</sup> However, these require manual inversion for underside seeding and are not compatible with high-throughput, multiplexed examination of compounds, donors, and recruitment conditions. 12- and 24-well assays also require high neutrophil numbers (millions/well) and clinical specimen volumes (milliliters/well) that constrain the amount of conditions that can be tested with these limited, valuable materials. A 96-well format would require 25 times less volume in the lower chamber per replicate, and at least 5 times less neutrophils per replicate. A 96-well Transwell<sup>®</sup> array is commercially available (Corning, HTS Transwell<sup>®</sup> 96-well Permeable Support), but bilayer co-culture on the Transwell-96 is hardly reported because underside cell seeding is prohibitively difficult at this minuscule filter size.<sup>40</sup> Cell-free and trans-endothelial recruitment in the Transwell-96 are reported more often,<sup>41,42</sup> but sacrificing either cell type is highly undesirable; both are critical participants in pulmonary neutrophil recruitment.<sup>43,44</sup> Taken together, the available neutrophil recruitment assays must compromise between clinical sample efficiency, throughput, physiologic relevance, ease of use, and availability of downstream analyses. These limiting compromises motivate novel approaches to meeting these conflicting technical demands to advance studies of neutrophilic inflammation.

Therefore, we report a novel assay, termed the 96-well leukocyte recruitment in an air-blood barrier array (L-ABBA-96), that precisely quantifies neutrophil number and activation status before and after endothelial-to-epithelial recruitment in a miniature, high-throughput format coupled to automated flow cytometry for immunophenotyping. The L-ABBA-96 builds off of our recently described method for underside epithelial seeding and bilayer co-culture with endothelial cells on the Transwell-96.<sup>40</sup> Healthy donor neutrophils placed in the endothelial chamber extravasate physiologically through the air-blood barrier toward chemoattractants in the epithelial chamber. We show that neutrophils recruited to IL-8 become activated by exposure to the epithelial milieu and acquire a phenotype similar to airway neutrophils *in vivo*. Interestingly, non-recruited endothelial neutrophils also acquire a physiologically relevant phenotype, mimicking the priming seen in circulating neutrophils. We then show that the immunomodulator baricitinib, JAK1/2 inhibitor recently Food and Drug Administration (FDA)-approved to treat Coronavirus Disease 2019 (COVID-19)-associated inflammation,<sup>45</sup> reduces neutrophil recruitment and shifts activation marker expression for both air- and blood-side neutrophils.<sup>46</sup> Finally, the L-ABBA-96 recapitulates cystic fibrosis inflammation; epithelial-side patient-derived sputum caused upregulation of e-selectin shifted surface markers to CF-mimetic phenotypes in both recruited and non-recruited neutrophils.

In summary, the L-ABBA-96 substantially improves the physiologic relevance of convenient and accessible plate-based transmigration assays and increases the volume of information gained from them by enabling traditional immunophenotyping and precise, high-throughput quantitation with automated flow cytometry. Accessibility of highly physiological and high-throughput assays to those not specialized in bioengineering is critical to advancing the field’s understanding of pulmonary inflammation and the development of neutrophil immunomodulators.

## RESULTS

### IL-8 and LTB<sub>4</sub> dose-dependently recruit primary human neutrophils in L-ABBA-96

Neutrophil recruitment from the circulation is a key event that sets the stage for tissue responses early after injury or infection.

Chemotaxis and transmigration, as well as soluble signals, prime quiescent circulating neutrophils for their eventual antimicrobial and pro-tissue regenerative functions once they arrive at the injury site.<sup>19,47,48</sup> Priming is followed by activation during transmigration, via engagement with endothelial, interstitial, and epithelial ligands; sensing of chemoattractants, extracellular matrix, and cytokines; and experiencing mechanical forces while squeezing through tissue.<sup>32,49–53</sup> Once reaching the site of injury, activated neutrophils release antimicrobial effectors, growth factors, cytokines, chemokines, and exosomes that influence the tissue microenvironment.<sup>54</sup> Therefore, rather than studying neutrophils isolated from blood, incorporating the key activating process of transmigration is critical to understanding neutrophilic inflammation and designing effective, targeted therapeutics to modulate it. The L-ABBA-96 aims to recapitulate these key *in vivo* steps of neutrophil priming, recruitment, and activation in a high-throughput *in vitro* platform [Figs. 1(a) and 1(b)]. Airway epithelial cells are seeded on the underside of Transwell membranes as previously described,<sup>40</sup> opposite to a confluent human endothelium. Chemoattractant is added to the lower epithelial compartment, and neutrophils are added to the upper endothelial compartment. Over several hours, neutrophils

transmigrate through the endothelium, the collagen-coated Transwell membrane, and the air-liquid interface-differentiated epithelium to reach the chemoattractant.

To establish quality control for transmigration assays, we optimized and standardized the L-ABBA-96 culture protocol to minimize edge position effects, a frequent concern with plate-based assays.<sup>55</sup> Controlling temperature and humidity prevented edge position effects on barrier strength, as measured by trans-epithelial/endothelial electrical resistance (TEER) (supplementary material, Fig. 1, Supplemental Method 1). Plates with an average TEER  $\geq 200 \Omega \cdot \text{cm}^2$  showed a negligible correlation between air-blood barrier strength in the numbers of recruited neutrophils (Supplemental Method 2; supplementary material, Figs. 2 and 3). With standard operating procedures and quality control metrics in place, we first analyzed recruitment of primary, human circulating neutrophils to increasing doses of the chemoattractants IL-8 and LTB4 [Fig. 1(d)]. The assay's throughput accommodates an eightfold dose-response curve with multiple donors, replicates, and chemoattractants, which minimizes experimental batch effects and improves the assay's resolution. We detected a significant difference between two independent donors in the dose-response curve for LTB4 ( $p < 0.0001$ ),

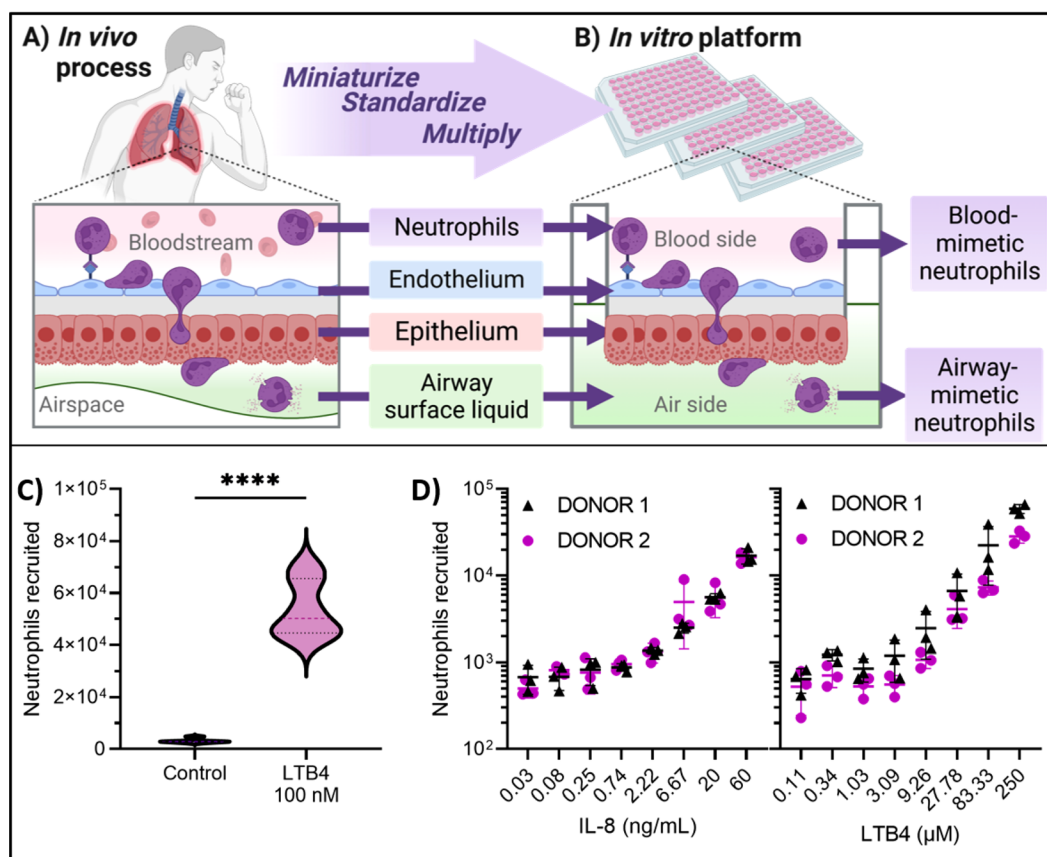


**FIG. 1.** A miniaturized air-blood barrier array recapitulates transendothelial-trans-epithelial neutrophil recruitment *in vitro*. Neutrophil recruitment to the distal lungs through the endothelium and then epithelium (a) is recapitulated in a miniaturized, standardized platform in 96-well format (b) using off-the-shelf reagents and standard cell culture equipment. (c) Despite miniaturization, neutrophils are recruited in high numbers with a high degree of specificity between negative and positive control conditions.  $n = 6$  per condition (3 replicates per donor, 2 donors). Compared with Student's *t*-test. \*\*\*\* $p < 0.0001$ . (d) Neutrophils are dose-dependently recruited to IL-8 and LTB4, two central chemoattractants in human lung diseases. The assay's high sensitivity and many replicates enable detection of a difference in the response to LTB4, but not IL-8, between two donors, according to two-way ANOVA ( $p < 0.0001$ ).  $n = 6$  per condition (3 replicates per donor, 2 donors). Figure created with BioRender software.

but not IL-8 ( $p = 93.97$ ) using a two-way ANOVA for the effects of chemoattractant and donor on the number of recruited neutrophils. While the effect is minor and secondary to the demonstration of precise and controlled dose-responses in the assay, it is interesting to note that the human LTB4 receptor is exceptionally epigenetically variable<sup>56</sup> and could cause biological variability in neutrophil responses between donors that are captured by the L-ABBA-96.

### L-ABBA-96 mimics activation marker shifts induced by lung neutrophil recruitment

The L-ABBA-96 platform recovers sufficient neutrophils for flow cytometric analysis (Gating scheme is shown in the [supplementary material](#), Fig. 4) for both unmigrated (top chamber) and migrated (bottom chamber) cells [Fig. 2(a)]. Thus, it enables evaluation of surface marker expression at 3 critical stages: (i) on freshly blood-isolated neutrophils immediately before placement in the assay; (ii) on unmigrated neutrophils (endothelial side); and (iii) on migrated neutrophils (epithelial side) accumulated at the air-blood barrier for the duration of the assay. We compared surface expression of key neutrophil phenotypic markers CD62L, CD16, CD66b, and CD63 after 14-h exposure of endothelial-side neutrophils to epithelial-side IL-8 (20 ng/mL), between 3 independent donors. Similar neutrophil numbers were recruited across the 3 donors ( $p = 0.19$ , one-way ANOVA with post-hoc Tukey's test) [Fig. 2(b)]. For all donors, neutrophil surface expression of CD62L, CD16, CD66b, and CD63 was consistent with quiescent, primed, and activated phenotypes of blood, unmigrated, and migrated neutrophils, respectively. For each marker, differences were assessed by two-way ANOVA between donor and condition with post-hoc Tukey's test for main row effect (i.e., averaged donors). CD62L is shed by enzymes during neutrophil priming<sup>47</sup> and further by ectodomain shedding by endothelial and epithelial disintegrins during transmigration<sup>57,58</sup> in line with our observations [Fig. 2(d-i)]. CD16 (Fc $\gamma$ RIIb) can be shed during priming, activation, and chemotaxis,<sup>59–61</sup> but it is also mobilized from intracellular stores during transmigration.<sup>61,62</sup> Our assay suggests unmigrated neutrophils were primed, reflected by decreased CD16 and then recovered expression with the stimulus of transmigration [Fig. 2(d-ii)]. CD66b and CD63, indicative of secondary and azurophilic degranulation, respectively, were only increased in the migrated neutrophils (although Donor 1 CD63 was not increased), suggesting migration stimulates activation and subsequent degranulation [Figs. 2(d-iii)–2(d-iv)].<sup>8</sup>

These observations suggest that the L-ABBA-96 captures key features of the physiologic cascade of neutrophil recruitment in the lung,<sup>63</sup> wherein neutrophils are quiescent in the bloodstream, primed during endothelial arrest and/or exposure to certain inflammatory signals,<sup>64</sup> and activated after transmigration to the lumen.<sup>63</sup> Interestingly, while neutrophil recruitment to IL-8 did not reveal a statistically different donor effect on neutrophil number (similar to in Fig. 1), flow cytometric quantitation of activation markers appears to reveal activation phenotype-based donor effects. According to two-way ANOVA analyzing the effect of transmigration (blood-isolated, unmigrated, or migrated) and donor-dependent biological variability in neutrophils, donor variation accounted for  $23.6 \pm 19.3\%$  of variation, on average, in the expression of surface markers ([supplementary material](#), Tables 1 and 2). Transmigration condition (blood-isolated, unmigrated, and migrated) accounted for the majority ( $62.1 \pm 25.3\%$ ) with minor interaction effects comprising the remainder ( $10.7 \pm 4.4$ ). These results underscore our platform's ability to

monitor neutrophil through various steps of priming and activation that accompany the transmigration process.

We also analyzed the response of neutrophils from a single donor to IL-8 (20 ng/mL), LTB4 (100  $\mu$ M), or control (epithelium submerged in media with no additional chemoattractant) using the same activation markers [Fig. 2(e)]. Transmigration effects were statistically significant ( $p < 0.001$ , two-way ANOVA) for all markers except CD63 ( $p = 0.1548$ ), which was not increased by recruitment to any chemoattractant for this particular donor. Taken together, the L-ABBA-96 induces neutrophil priming, recruitment, and activation and quantifies the changes with sufficient resolution, consistency, and number of replicates that biological variability of response from different donor neutrophils or chemoattractants can be discerned.

### Baricitinib dose-dependently inhibits neutrophils' recruitment and modulates their surface phenotype

We then evaluated the influence of baricitinib, a small-molecule JAK1/2 inhibitor, on IL-8-driven neutrophil recruitment in a model of severe pulmonary inflammation.<sup>65</sup> Baricitinib was recently approved by the U.S. Food and Drug Administration for controlling pulmonary inflammation in severe Coronavirus Disease 2019 (COVID-19) and is a promising immunomodulator for many other inflammatory lung diseases.<sup>45,65–69</sup> We used IL-8 alone at 20 ng/mL, a high concentration similar to that in bronchoalveolar lavage fluid from patients with severe COVID-19.<sup>70,71</sup> Figure 3(a) shows log–log plots of number of neutrophils vs the baricitinib dose for a combined  $N = 5$  donors across 9 assays, demonstrating a small ( $r^2 = 0.2781$ ) but robust ( $p < 0.0001$ ) linearized dose-dependent reduction in recruited neutrophils [Fig. 3(a)]. Interestingly, reduced neutrophil recruitment was also observed in rhesus macaques treated with baricitinib for COVID-19,<sup>72</sup> supporting our assay's unique sensitivity and physiologic relevance. Additionally, the half maximal inhibitory concentration (IC50) of baricitinib varied widely across 3 neutrophil donors tested on the same L-ABBA-96 assay plate (1.409  $\mu$ M, 1.86  $\mu$ M, and 95.9 nM) ([supplementary material](#), Fig. 5). These IC50 values may be explained by the fact that IL-8 mediates chemotaxis through JAK3 rather than baricitinib's main targets JAK1/2.<sup>73</sup> Cell-free assays determined baricitinib's IC50 against JAK1 and JAK2 as 5.9 and 5.7 nM, respectively, and  $\sim 420$  nM for JAK3,<sup>65</sup> which is within one order of magnitude of our measured IC50s for neutrophil recruitment inhibition. Interestingly, maximum plasma concentration of baricitinib is  $97.5 \pm 21.6$  nM ( $36.2 \pm 8.0$  ng/mL),<sup>74</sup> close to the IC50 determined for one donor in the L-ABBA-96 (95.9 nM), suggesting that current clinical dosing strategies could be sufficient to inhibit neutrophil recruitment *in vivo*. Interestingly, baricitinib reduces neutrophil recruitment to the lungs in rhesus macaques infected with COVID-19.<sup>72</sup>

Additionally, a population of highly active, immunosuppressive neutrophils with a CD62L<sup>dim</sup>CD16<sup>bright</sup> phenotype has recently been identified in COVID-19 and other inflammatory conditions.<sup>75–78</sup> In the L-ABBA-96, baricitinib dose-dependently reduced the proportion of IL-8-induced CD62L<sup>dim</sup>CD16<sup>bright</sup> neutrophils in both unmigrated and migrated populations (Gating strategy with no baricitinib treatment, [supplementary material](#), Fig. 6). Conversely, with increasing baricitinib dose, CD62L was shed more in unmigrated neutrophils, and CD16 was shed more in both unmigrated and migrated neutrophils. This suggests that baricitinib may enhance priming of unmigrated neutrophils, through an as yet unknown mechanism. Interestingly, CD66b and CD63 were not significantly impacted in either



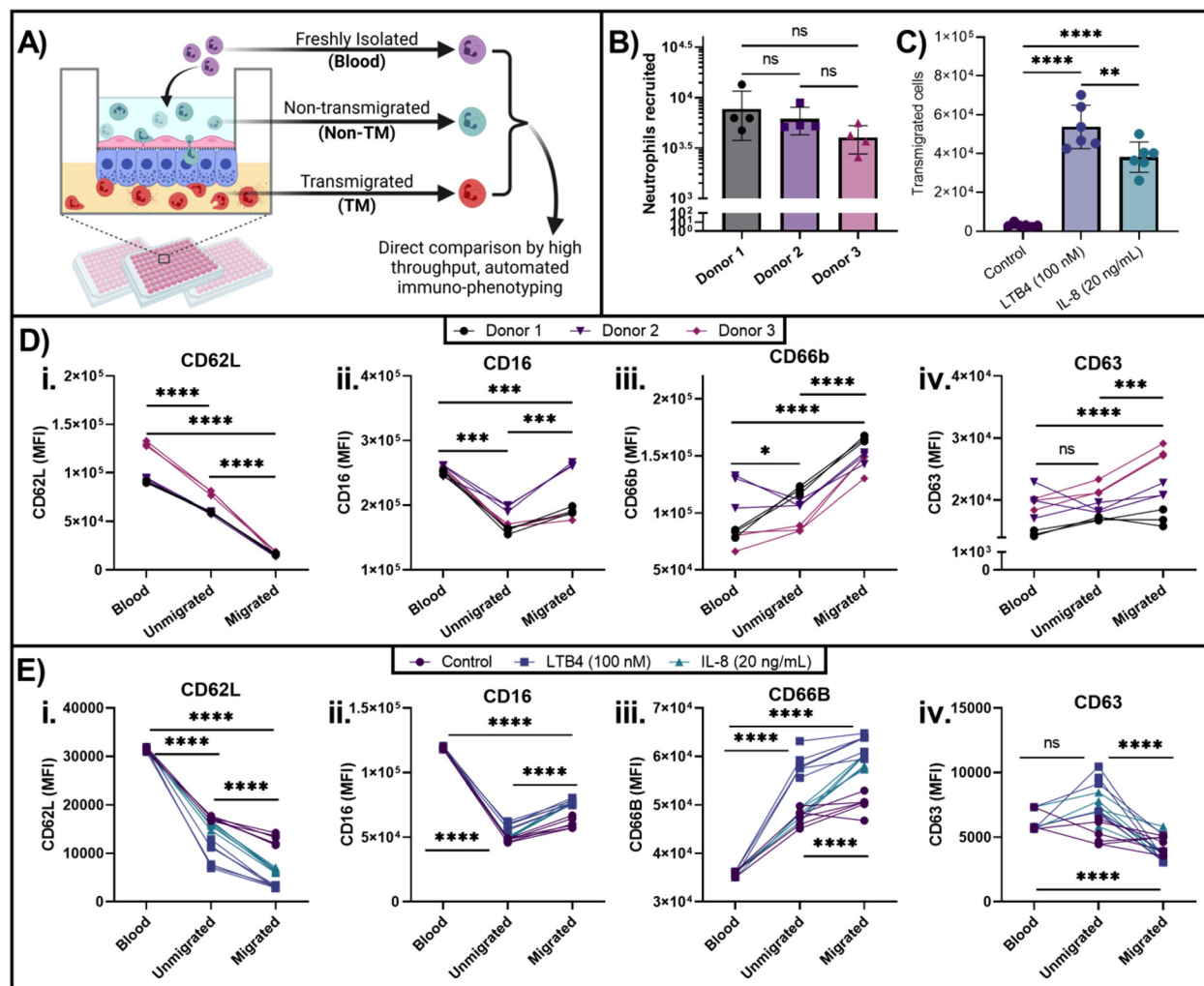


**FIG. 2.** Neutrophil recruitment *in vitro* reflects physiologic shifts in key surface markers. (a) Key activation markers CD62L, CD66b, CD16, and CD63 were compared between blood, untransmigrated, and transmigrated neutrophils across 3 donors for 1 chemoattractant (b) and (d) and 3 chemoattractant conditions for 1 donor (c) and (e). (b) and (d) Neutrophils were recruited to epithelial IL-8 (20 ng/mL), LTB4 (100 nM), or no chemoattractant for 14 h ( $n = 4$ –6 replicates/donor). (b) Comparable numbers of neutrophils from each donor are recruited to IL-8 (20 ng/mL). (c) LTB4 (100 nM) attracts more neutrophils than IL-8 (20 ng/mL). (d-i) and (e-i) CD62L, or L-selectin, is shed during priming, and further by transmigration, due to engagement with endothelial and epithelial disintegrins, across donors and recruitment conditions. (d-ii) and (e-ii) CD16 (Fc $\gamma$ R/III) is shed during priming and activation of neutrophils, as in the non-TM population, but can be replaced by intracellular reserves after transmigration, which is consistent with the increase seen in TM neutrophils in our assay for multiple donors and chemoattractants. (d-iii) and (e-iii) CD66b is a human-specific marker of neutrophil degranulation associated with activation. Physiologic recruitment to the lung increases CD66b, and this is captured in our assay across donors and chemoattractants. LTB4 activates non-recruited neutrophils more than IL-8. (d-iv) and (e-iv) Degranulation of azurophilic granules, represented by CD63, indicates neutrophil activation, which is mildly induced in certain donors by recruitment to large concentrations of chemoattractant, such as the 20 ng/mL IL-8 used here. Interestingly, CD63 was not increased for the single donor across conditions, suggesting donor effects. (b)  $N = 3$  donors,  $n = 4$  replicates/donor; (d)  $N = 3$  donors,  $n = 3$  replicates/donor; (c) and (e)  $N = 1$  donor,  $n = 3$  replicates/condition. (b) and (c) One-way ANOVA with post-hoc Tukey's test. (d) and (e) Analyzed by two-way ANOVA with post-hoc Tukey's test (main row effect). \* $p < 0.05$ , \*\* $p < 0.01$ , \*\*\* $p < 0.001$ , \*\*\*\* $p < 0.0001$ . (a) was created with BioRender.

unmigrated or migrated neutrophils, suggesting no significant degranulation is induced until a dose of baricitinib of 6.25  $\mu$ M, which is two orders of magnitude greater than its reported maximal serum concentration of around 100 nM.<sup>74</sup> The clinically relevant 98 nM dose in our study was enough to significantly reduce the proportion of CD62L<sup>dim</sup>CD16<sup>bright</sup> neutrophils among untransmigrated neutrophils without inducing appreciable activation [Figs. 3(c)–3(f)]. Taken together, baricitinib in the L-ABBA-96 dose-dependently attenuates neutrophil

recruitment and induction of the pathological CD62L<sup>dim</sup>CD16<sup>bright</sup> phenotype.

### Recruitment to cystic fibrosis sputum-derived airway supernatant induces disease-mimetic inflammatory phenotypes

To demonstrate the capability of the L-ABBA-96 to capture disease-specific pathophysiology, the L-ABBA-96 epithelium was

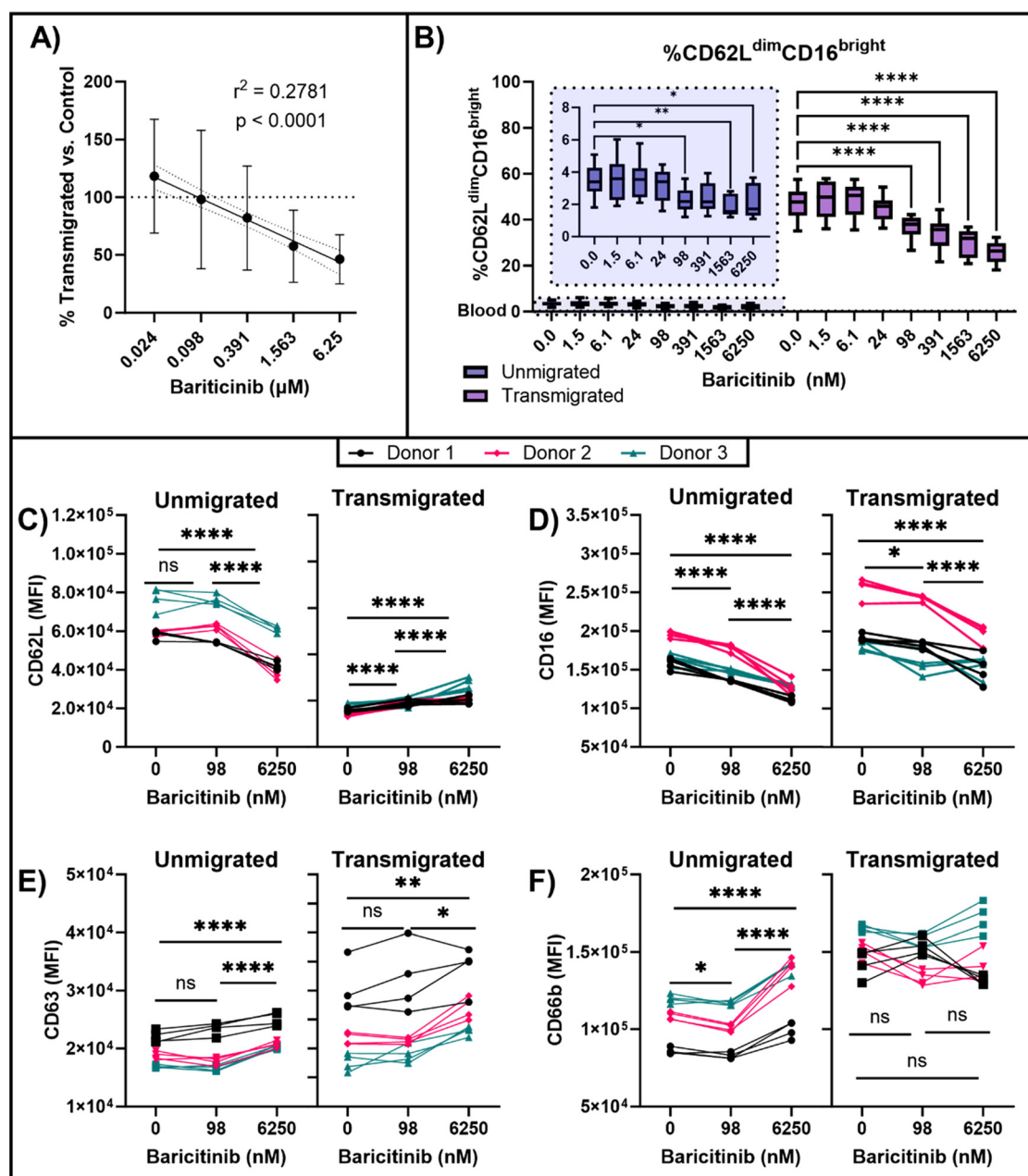


**FIG. 3.** Baricitinib on the endothelial side of the L-ABBA-96 dose-dependently modulates neutrophil phenotype. (a) Across 5 donors and 9 assays, baricitinib significantly reduced neutrophil recruitment toward IL-8 (20 ng/mL). A simple linear regression of the linearized data revealed a weak ( $r^2 = 0.2781$ ) yet highly significant ( $p < 0.0001$ ) negative correlation between drug concentration and recruited neutrophil number.  $N = 5$  donors,  $n = 3$ –6 replicates/donor/assay. (b) Highly activated CD62L<sup>dim</sup>CD16<sup>bright</sup> neutrophils are attenuated by baricitinib on the blood side (inset, repeated measures one-way ANOVA with Dunnett's post-hoc test) and the air side (two-way ANOVA with post-hoc Dunnett's test against zero drug control, matched by well for TM and non-TM).  $N = 3$  donors,  $n = 4$  replicates/donor. (c)–(f) A non-physiologically relevant dose of 6250 nM baricitinib induced mild priming and activation that was negligible at a clinically relevant dose of baricitinib (98 nM). Two-way ANOVA with post-hoc Tukey's test (main row effect). Within unmigrated or transmigrated. \* $p < 0.05$ , \*\* $p < 0.01$ , \*\*\* $p < 0.001$ , \*\*\*\* $p < 0.0001$ .

exposed to pooled human cystic fibrosis (CF) sputum-derived airway supernatant<sup>37</sup> (CFASN) [Fig. 4(a)]. Previous Alvetex-based recruitment experiments by our group show that trans-interstitial and epithelial migration into CFASN programs neutrophils toward

disease-characteristic features of granule-releasing, immunomodulatory and metabolically active ("GRIM") cells, with low bacterial killing.<sup>37</sup> GRIM neutrophils present in the CF lung lumen are CD62L<sup>dim</sup> due to transmigration,<sup>58</sup> CD66b<sup>bright</sup> and CD63<sup>bright</sup> due to high

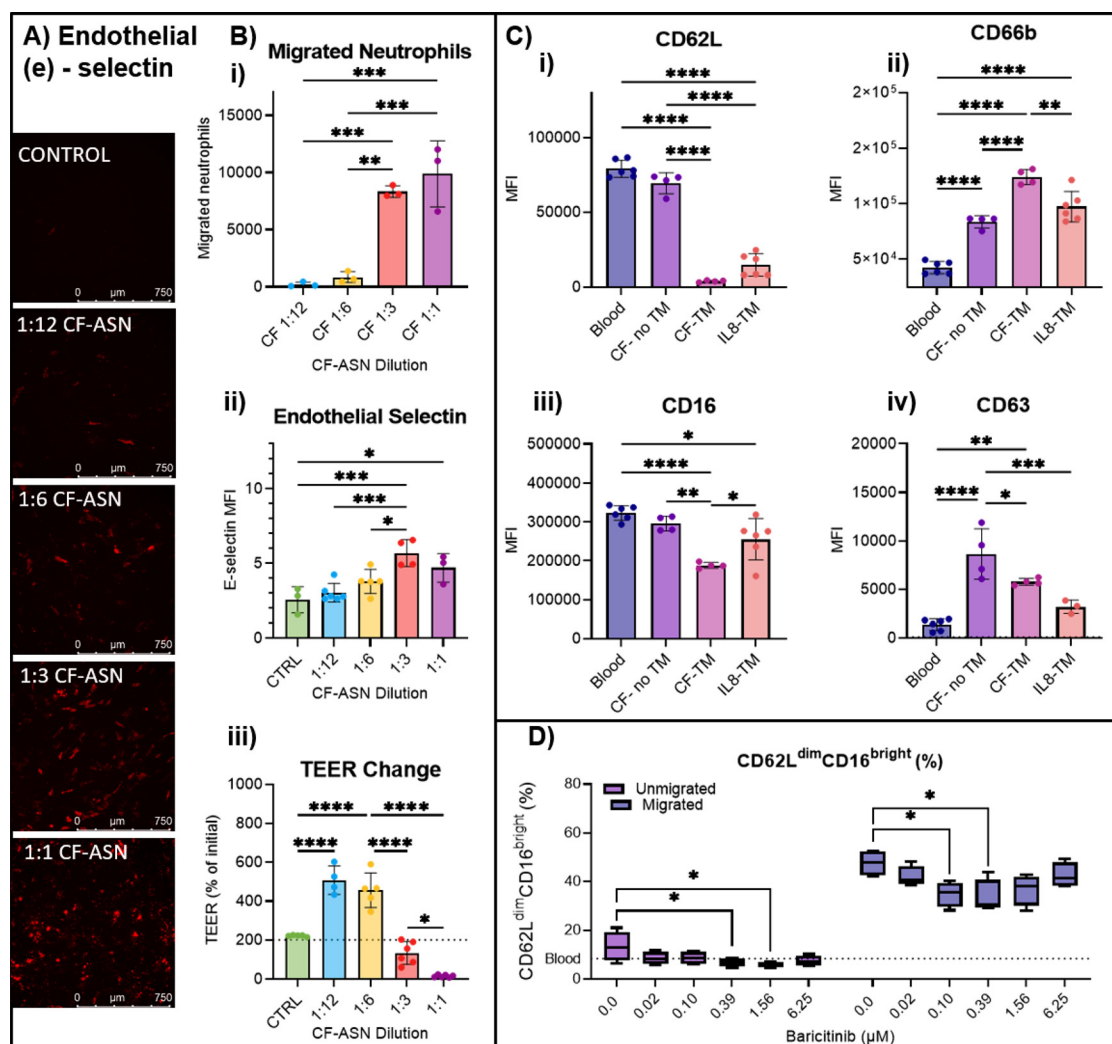


**FIG. 4.** L-ABBA-96 recapitulates pulmonary neutrophilia and elevated blood neutrophil activation characteristic of cystic fibrosis. Healthy donor neutrophils were recruited toward pooled, patient-derived CF-ASN containing the soluble factors from sputum without mucus or cells. Lung-recruited CF neutrophils demonstrate significant activation and characteristically lose CD62L and CD16 while gaining CD66b and CD63. (a) Endothelial selectin (e-selectin) was upregulated on endothelial cells in the L-ABBA-96 after 18 h' exposure to epithelial-side CF-ASN [quantified in (b-ii)]. (b-i) Neutrophils migrate dose-dependently to CF-ASN. (b-ii) E-selectin protein is upregulated dose-dependently by CF-ASN on the epithelium according to quantitative immunofluorescence. (b-iii) Epithelial-endothelial barrier strength, measured by TEER, is compromised by high concentrations of CF-ASN. (c) Neutrophils recruited to CF-ASN (hereafter CF-TM neutrophils) display more activation than those recruited to IL-8 (IL8-TM). (c-i, c-ii, c-iii, and c-iv) CF-TM neutrophils trend toward losing more CD62L and gaining more CD66b than IL8-TM. They statistically lose more CD16 and gain more CD66b than IL8-TM. (d) Unmigrated and migrated neutrophil proportion of CD62L<sup>dim</sup>CD16<sup>bright</sup> is dose-dependently reduced by baricitinib. All except (d) were analyzed by one-way ANOVA with post-hoc Tukey's test. (d) Two-way ANOVA with post-hoc Tukey's test. (c) Two donors, 2–3 replicates/donor; (d) 2 donors, 2 replicates/donor. \* $p < 0.05$ , \*\* $p < 0.01$ , \*\*\* $p < 0.001$ , \*\*\*\* $p < 0.0001$ .

release of secondary and primary granules (the latter containing neutrophil elastase), and simultaneously CD16<sup>dim</sup> due cleavage by elastase.<sup>37</sup> Here, in the L-ABBA-96, neutrophils were allowed to transmigrate for 18 h into CFASN (or IL-8 at 20 ng/mL as a control), diluted in cell culture medium at a ratio between 1:12 and 1:1, as specified. Neutrophils transmigrated dose-dependently to increasing concentrations of CFASN. Interestingly, TEER increased and decreased at low and high CFASN concentrations, respectively [Fig. 4(a)]. The endothelium also upregulated E-selectin following exposure to CF-ASN in

the epithelial compartment in a dose-dependent manner [Fig. 4(b)]. Consistently, CF patient serum contains elevated soluble E-selectin.<sup>79,80</sup>

Next, we evaluated the mobilization of surface markers [Fig. 4(c)] on neutrophils from the CFASN-treated L-ABBA-96. We excluded the 1:12 and 1:6 conditions due to low transmigrated cell numbers. At the higher concentration CFASN conditions, the transmigrated neutrophils shed CD16 and gained CD66b significantly more than neutrophils recruited to IL-8 in the same assay. Recruited CF neutrophils also trended toward lower CD62L and higher CD63 than recruited

IL-8 neutrophils, although significance was not achieved by one-way ANOVA.<sup>81</sup> Overall, the greater activation indicated by the surface markers measured is consistent with a CF-like activation of recruited neutrophils.

Interestingly, unmigrated (blood-side) neutrophils also displayed a CF-like phenotype in the L-ABBA-96. CF patients have an elevated proportion of circulating CD62L<sup>dim</sup>CD16<sup>bright</sup> neutrophils,<sup>82</sup> which was reflected in the CF-ASN exposed L-ABBA-96 [Fig. 4(d)]. As previously mentioned, this population has been characterized as immunomodulatory and highly activated in acute inflammation, but their role in CF is not well characterized.<sup>75,83</sup> CF patients circulating neutrophils are approximately 20% CD62L<sup>dim</sup>CD16<sup>bright</sup>; in the L-ABBA-96, a similar proportion ( $13.2 \pm 5.3\%$ ) of neutrophils were CD62L<sup>dim</sup>CD16<sup>bright</sup> despite originating from healthy donors and failing to develop this magnitude of a response to IL-8 (20 ng/mL) during the same assay.<sup>82</sup> Furthermore, this population on both air and blood sides were reduced by clinically relevant doses of baricitinib, mirroring results from Fig. 3 for recruitment to IL-8. In summary, the L-ABBA-96 recapitulates multimodal features of CF pulmonary inflammation, including neutrophilia, e-selectin upregulation, significant recruitment-induced activation, and the appearance of a blood-side population of CD62L<sup>dim</sup>CD16<sup>bright</sup> neutrophils at a similar proportion to human patients, supporting its value for disease-specific investigations.

## DISCUSSION

Current methods for *in vitro* assessment of human neutrophil-driven lung inflammation are limited in throughput, standardization, phenotypic relevance, or ability to recover sufficient numbers of cells to perform high-content phenotypic analyses. Here, we bridge this gap with a high-throughput, miniaturized assay comprised of an array of leukocyte-laden air-blood barriers, the L-ABBA-96, that can be coupled with multifactorial outcome quantification of airway barrier function and neutrophil phenotype by flow cytometry. Quantification of these parameters across more than a thousand air-blood barriers demonstrates reproducibility and consistency across different wells, plates, neutrophil donors as well as versatility across a variety of stimulants, including chemoattractants, cytokines, and patient fluid samples.

The L-ABBA-96 benefits from operating at the meso-scale, between microfluidics and traditional plate-based assays. This allows recovery of adequate numbers of cells (>1000s transmigrated cells) from each well of 96-well format plates in a manner compatible with high-throughput flow cytometry while being volume efficient (<100  $\mu$ L per bottom well) to minimize use of clinical specimens and costly reagents. Indeed, most plate-based assays do not offer tissue-level complexity and miniaturization, as these features are typically reserved for microfluidic devices. As opposed to microfluidics, however, our platform requires similar technical complexity, skill, and equipment to existing plate-based transmigration assays that are widely used. Our platform also excludes the use of glucocorticoids commonly used to stimulate epithelial differentiation.<sup>84</sup> Therefore, we are able to study inflammation-modulating therapies without interference.

Detailed dose-response studies of neutrophil recruitment and activation across multiple donors are uncommon, at least in part, due to technical limitations such as low throughput or limited numbers of transmigrated cells hampering downstream analyses. The L-ABBA-96 accommodates eightfold dose-response curves on a single plate with many replicates to increase confidence while reducing experimental

variability. Each replicate has 3 interacting cell types, epithelial-side exposure to chemoattractants or clinical samples, the endothelial side is dosed with different concentrations of a therapeutic, and outcomes quantified through TEER and flow cytometry of unmigrated (blood-side) and transmigrated (airway-side) neutrophils. The procedures are amenable to scale-up and automation using off-the-shelf cultureware, liquid handlers, and measurement systems including underside epithelial seeding, leukocyte loading and transmigration, barrier property measurement, and flow cytometry. In regard to leukocyte loading, we added in this study a number of neutrophils per surface area of endothelium that is in line with prior studies ( $\sim 1.7 \times 10^6$  per  $\text{cm}^2$ ), but this number can easily be increased or decreased, depending on modeling needs. These unique advantages position the L-ABBA-96 to characterize pulmonary insults such as inhalants from cigarettes, e-cigarettes, and other electronic nicotine delivery systems using novel immune-relevant outcome measures that may relate to pathophysiology.

Another key feature of the L-ABBA-96 is its ability to recover unmigrated neutrophils that remain on the endothelium but can, nonetheless, alter their phenotype in response to epithelial-side stimulation. Interestingly, blood-side neutrophils in the L-ABBA-96 developed a CD62L<sup>dim</sup>CD16<sup>bright</sup> phenotype reported as pathologic in systemic inflammatory conditions such as endotoxin challenge<sup>75</sup> and cancer.<sup>85</sup> Most recently, an elevated CD62L<sup>dim</sup>CD16<sup>bright</sup> neutrophil count in COVID-19 patients was associated with developing pulmonary embolism.<sup>77</sup> Unexpectedly, in our assay, baricitinib dose-dependently reduced the proportion of CD62L<sup>dim</sup>CD16<sup>bright</sup> neutrophils among unmigrated and migrated neutrophils at clinically relevant doses. A recent case study reported the same effect of baricitinib on neutrophils in a COVID-19 patient.<sup>46,86</sup>

Compared to sophisticated lung-on-a-chip systems, the L-ABBA-96 has limitations in lacking physiological flow over the endothelium, pathophysiological fluid mechanical stress on the epithelium, as well as stretch. Compared to the Alvetex system that has a thicker interstitium with a complex geometry to represent later stage disease and promote neutrophil activation by collagen interactions and autocrine signaling, the L-ABBA-96 only has a thin collagen-coated porous membrane as the interstitium. Additionally, epithelial and endothelial cell types could be primary human lung-derived cells rather than cell lines or pooled umbilical vein cells. Beyond the lung, other mucosa-blood barriers that experience pathological neutrophil recruitment (e.g., the gut, skin, and oral, nasal mucosae) can be modeled in the L-ABBA-96 by exchanging the epithelial cells, expanding the platform's impact.

Regardless, the L-ABBA-96 has strengths in using commercially available cultureware, readily available tools and reagents, and interfacing seamlessly with common automated flow cytometers, making it widely accessible and immediately adaptable by all for further applications and improvements. While the biological findings of the work presented serve to demonstrate the capabilities and disease relevance of our platform, they also represent a significant technological advance for lung inflammation studies.

## METHODS

### Preparation of air-blood barrier array (ABBA)

The ABBA was prepared in a standardized protocol as previously described by our group.<sup>40</sup> Briefly, we seeded human small airway-like epithelial cell line NCI-H441 [American Type Culture Collection (ATCC)] on the underside of the Transwell<sup>®</sup> membrane (Corning



HTS Transwell® 96-well Permeable Support, polycarbonate, 3  $\mu$ m pore size, #3386) using flotation. The endothelium was modeled with primary human umbilical vein endothelial cells (HUVECs, ATCC) that were pooled from multiple donors to reduce donor-specific variation.

### Neutrophil transmigration assays

Human peripheral blood was obtained through venipuncture under Georgia Tech Institutional Review Board (IRB)-approved protocols and isolated by negative selection according to the manufacturer's instructions (Miltenyi Biotec 130–104–434, 130–098–196). Trans-epithelial electrical resistance was measured as previously described with the EVOM2 and STX HTS for Corning 96 (World Precision Instruments).<sup>40</sup> Chemoattractants (leukotriene B<sub>4</sub>, Cayman Chemical #20110; Interleukin 8, MyBioSource #MBS9718666) were prepared at the specified concentrations in the air-liquid interface (ALI) medium as described previously.<sup>40</sup> In CFASN assays, pooled patient airway supernatant obtained under an Emory IRB-approved collection was prepared as described,<sup>87</sup> diluted in ALI media to various concentrations as specified, and placed in the receiver plate. In drug testing assays, isolated neutrophils were suspended in media containing specified drug concentrations (baricitinib, Cayman Chemical #16707). Media was completely removed from the top chamber of the Transwell inserts, and neutrophils suspended in the ALI medium were placed in the top chamber of the Transwell at 100  $\mu$ L/well, with 225 000–330 000 cells/well depending on the experiment. Neutrophils were placed in the top chamber, and inserts were placed immediately into pre-warmed receiver plate containing the chemoattractant or patient specimen. The plate was incubated for 16 h at 37 °C, 95% humidity, 5% CO<sub>2</sub>.

### Flow cytometry

Freshly isolated neutrophils were stained for flow cytometry immediately after isolation in a FACS tube. Transmigrated neutrophils were collected into non-tissue culture treated round-bottom 96-well plates, blocked with Human TruStain FcX™ (Fc block, compatible with anti-CD16 staining) and stained according to optimized panels (supplementary material, Table 3). Flow cytometry was performed using a Cytoflex S (Beckman Coulter) at 30  $\mu$ L/min. Compensation was collected using single-antibody stained Abc Beads for antibodies and Arc beads for live/dead according to the manufacturer's instructions. Gating and compensation matrix was performed in FlowJo (BD Biosciences). Cell quantitation and median fluorescence intensities (MFIs) for given markers were calculated using FlowJo. Gating strategy is described in the supplementary material, Fig. 3.

### Statistical analysis

All statistics were performed in GraphPad Prism 10.1.2. All significance tests were performed with  $\alpha = 0.05$  (95% confidence). Figure 1(c): Student's t-test (unpaired); Fig. 1(d): two-way ANOVA; Figs. 2(b) and 2(c): ordinary one-way ANOVA with post-hoc Tukey's test; Figs. 2(d) and 2(e): two-way ANOVA with post-hoc Tukey's test for main row effect (i.e., averaged donors or chemoattractants); Fig. 3(a): simple linear regression with 95% confidence intervals (dotted lines) and standard deviations (error bars); Fig. 3(b) (inset): ordinary one-way ANOVA with post-hoc Tukey's test; Fig. 3(b) (non-inset):

two-way ANOVA with post-hoc Dunnett's test against control; Figs. 3(c)–3(f): two-way ANOVA with post-hoc Tukey's test for main row effect (i.e., averaged donors); Figs. 4(b) and 4(c): ordinary one-way ANOVA with post-hoc Tukey's test; Fig. 4(d): two-way ANOVA with post-hoc Dunnett's test against control. For all graphs and charts, \* $p < 0.05$ , \*\* $p < 0.01$ , \*\*\* $p < 0.001$ , \*\*\*\* $p < 0.0001$ .

### SUPPLEMENTARY MATERIAL

See the [supplementary material](#) for data regarding edge effects, humidity chamber, flow gating strategies, and other details.

### ACKNOWLEDGMENTS

We thank blood donors who participated in this study, and the many other individuals who have contributed directly or indirectly to its implementation. This study was funded by R01HL136141 (National Institutes of Health), U.S. Food and Drug Administration (FDA) Center for Tobacco Products (CTP) (No. 75F40122C00146), Biomedical Engineering COVID Seed grant (Georgia Institute of Technology), and Georgia Tech EPICenter (Georgia Institution of Technology) to S.T.; 5T32EB006343-08 (National Institutes of Health) to H.V.; R01HL159058 (National Institutes of Health) and Cystic Fibrosis Foundation TIROUV22G0 to R.T.; K24 NR018866 (National Institutes of Health) to A.F.; and K23HL151897; R01HL171627 (National Institutes of Health) to J.G. We thank the GT IBB Core facilities for assistance with flow cytometry. This publication was developed in part under Assistance Agreement No. 84045201 awarded by the U.S. Environmental Protection Agency to ST & NLN. It has not been formally reviewed by EPA. The views expressed in this document are solely those of the authors and do not necessarily reflect those of the Agency. EPA does not endorse any products or commercial services mentioned in this publication.

### AUTHOR DECLARATIONS

#### Conflict of Interest

H.V., J.G., R.T., and S.T. are inventors on PCT/US22/18810, filed March 3, 2022, related to this work.

#### Ethics Approval

Ethics approval for experiments reported in the submitted manuscript on animal or human subjects was granted. De-identified human cystic fibrosis specimens were obtained by qualified clinicians in a clinical study approved by the Emory University Institutional Review Board (IRB00042577). Informed consent was obtained from all participants; however, because our study herein did not include identifiable human subjects, informed consent for the application of specimens to this particular study was not required. Human blood was obtained by the Lam Lab and Takayama Lab in clinical studies approved by the Georgia Institute of Technology Institutional Review Board (IRB Nos. H23498 and H23164, respectively). Informed consent to collect blood was obtained by all participants to participate in the study.

#### Author Contributions

Hannah Viola and Liang-Hsin Chen contributed equally to this work.

**Hannah Viola:** Conceptualization (equal); Data curation (equal); Formal analysis (equal); Funding acquisition (equal); Investigation (equal); Methodology (equal); Supervision (equal); Visualization (equal); Writing – original draft (equal); Writing – review & editing (equal). **Liang-Hsin Chen:** Data curation (equal); Formal analysis (supporting); Investigation (equal); Validation (equal); Writing – review & editing (equal). **Seongbin Jo:** Investigation (equal); Validation (equal); Writing – review & editing (supporting). **Kendra Washington:** Investigation (supporting); Validation (supporting); Writing – review & editing (supporting). **Cauviya Selva:** Investigation (supporting); Validation (supporting); Writing – review & editing (supporting). **Andrea Li:** Investigation (supporting); Validation (supporting); Writing – review & editing (supporting). **Daniel Feng:** Investigation (supporting); Validation (supporting); Writing – review & editing (supporting). **Vincent Giacalone:** Conceptualization (supporting); Methodology (supporting); Resources (equal); Writing – review & editing (supporting). **Susan T. Stephenson:** Validation (equal); Writing – review & editing (supporting). **Kirsten Cottrill:** Validation (supporting); Writing – review & editing (supporting). **Ahmad Mohammad:** Validation (supporting); Writing – review & editing (supporting). **Evelyn Williams:** Resources (lead); Writing – review & editing (supporting). **Xianggui Qu:** Formal analysis (supporting); Writing – review & editing (supporting). **Wilbur Lam:** Resources (supporting); Writing – review & editing (supporting). **Nga L. Ng:** Funding acquisition (equal); Supervision (supporting). **Anne Fitzpatrick:** Conceptualization (equal); Funding acquisition (supporting); Project administration (supporting); Resources (equal); Writing – review & editing (supporting). **Jocelyn Grunwell:** Conceptualization (equal); Funding acquisition (supporting); Methodology (equal); Project administration (supporting); Resources (equal); Writing – review & editing (supporting). **Rabindra Tirouvanziam:** Conceptualization (equal); Funding acquisition (equal); Methodology (equal); Project administration (equal); Resources (equal); Supervision (equal); Writing – review & editing (equal). **Shuichi Takayama:** Conceptualization (equal); Funding acquisition (equal); Methodology (equal); Resources (equal); Supervision (equal); Writing – review & editing (equal).

## DATA AVAILABILITY

The data that support the findings of this study are available from the corresponding authors upon reasonable request.

## REFERENCES

- <sup>1</sup>C. Summers, “Chasing the ‘Holy Grail’ – Modulating neutrophils in inflammatory lung disease,” *Am. J. Respir. Crit. Care Med.* **200**, 131–132 (2019).
- <sup>2</sup>T. Németh, M. Sperandio, and A. Mócsai, “Neutrophils as emerging therapeutic targets,” *Nat. Rev. Drug Discov.* **19**, 253–275 (2020).
- <sup>3</sup>M. A. Cruz *et al.*, “Nanomedicine platform for targeting activated neutrophils and neutrophil-platelet complexes using an  $\alpha 1$ -antitrypsin-derived peptide motif,” *Nat. Nanotechnol.* **17**, 1004–1014 (2022).
- <sup>4</sup>D. A. Amratia, H. Viola, and O. C. Ioachimescu, “Glucocorticoid therapy in respiratory illness: Bench to bedside,” *J. Invest. Med.* **70**, 1662 (2022).
- <sup>5</sup>S. Sinha *et al.*, “Dexamethasone modulates immature neutrophils and interferon programming in severe COVID-19,” *Nat. Med.* **28**, 201–211 (2022).
- <sup>6</sup>Y. Wang *et al.*, “Small-molecule modulators of toll-like receptors,” *Acc. Chem. Res.* **53**, 1046–1055 (2020).
- <sup>7</sup>M. Metzmaekers, M. Gouwy, and P. Proost, “Neutrophil chemoattractant receptors in health and disease: Double-edged swords,” *Cell. Mol. Immunol.* **17**, 433–450 (2020).
- <sup>8</sup>A. Othman, M. Sekheri, and J. G. Filep, “Roles of neutrophil granule proteins in orchestrating inflammation and immunity,” *FEBS J.* **289**, 3932–3953 (2022).
- <sup>9</sup>A. Margraf, C. A. Lowell, and A. Zarbock, “Neutrophils in acute inflammation: Current concepts and translational implications,” *Blood* **139**, 2130–2144 (2022).
- <sup>10</sup>J. Stackowicz, F. Jönsson, and L. L. Reber, “Mouse models and tools for the in vivo study of neutrophils,” *Front. Immunol.* **10**, 3130 (2020).
- <sup>11</sup>K. R. Patil *et al.*, “Animal models of inflammation for screening of anti-inflammatory drugs: implications for the discovery and development of phyto-pharmaceuticals,” *Int. J. Mol. Sci.* **20**, 4367 (2019).
- <sup>12</sup>K. Matsushima, D. Yang, and J. J. Oppenheim, “Interleukin-8: An evolving chemokine,” *Cytokine* **153**, 155828 (2022).
- <sup>13</sup>M. C. Cesta *et al.*, “The role of interleukin-8 in lung inflammation and injury: Implications for the management of COVID-19 and hyperinflammatory acute respiratory distress syndrome,” *Front. Pharmacol.* **12**, 808797 (2022).
- <sup>14</sup>D. Irimia and X. Wang, “Inflammation-on-a-chip: Probing the immune system ex vivo,” *Trends Biotechnol.* **36**, 923–937 (2018).
- <sup>15</sup>S. Han *et al.*, “A versatile assay for monitoring in vivo -like transendothelial migration of neutrophils,” *Lab Chip* **12**, 3861–3865 (2012).
- <sup>16</sup>D. Huh *et al.*, “Reconstituting organ-level lung functions on a chip,” *Science* **328**, 1662–1668 (2010).
- <sup>17</sup>K. Chew *et al.*, “A protocol for high-throughput screening for immunomodulatory compounds using human primary cells,” *STAR Protoc.* **4**, 102405 (2023).
- <sup>18</sup>D. Lv *et al.*, “A novel cell-based assay for dynamically detecting neutrophil extracellular traps-induced lung epithelial injuries,” *Exp. Cell Res.* **394**, 112101 (2020).
- <sup>19</sup>K. L. Vogt, C. Summers, E. R. Chilvers, and A. M. Condliffe, “Priming and de-priming of neutrophil responses in vitro and in vivo,” *Eur. J. Clin. Invest.* **48**(Suppl 2), e12967 (2018).
- <sup>20</sup>S. D. Kumar, K. Krishnamurthy, J. Manikandan, P. N. Pakeerappa, and P. N. Pushparaj, “Deciphering the key molecular and cellular events in neutrophil transmigration during acute inflammation,” *Bioinformatics* **6**, 111–114 (2011).
- <sup>21</sup>S. S. Hinman *et al.*, “Microphysiological system design: Simplicity is elegance,” *Curr. Opin. Biomed. Eng.* **13**, 94–102 (2020).
- <sup>22</sup>C. Probst, S. Schneider, and P. Loskill, “High-throughput organ-on-a-chip systems: Current status and remaining challenges,” *Curr. Opin. Biomed. Eng.* **6**, 33–41 (2018).
- <sup>23</sup>R. D. Kamm *et al.*, “Perspective: The promise of multi-cellular engineered living systems,” *APL Bioeng.* **2**, 040901 (2018).
- <sup>24</sup>H. Viola *et al.*, “Microphysiological systems modeling acute respiratory distress syndrome that capture mechanical force-induced injury-inflammation-repair,” *APL Bioeng.* **3**, 041503 (2019).
- <sup>25</sup>D. Huh *et al.*, “Acoustically detectable cellular-level lung injury induced by fluid mechanical stresses in microfluidic airway systems,” *Proc. Natl. Acad. Sci. U. S. A.* **104**, 18886–18891 (2007).
- <sup>26</sup>H. L. Viola *et al.*, “Liquid plug propagation in computer-controlled microfluidic airway-on-a-chip with semi-circular microchannels,” *Lab Chip* **24**(2), 197 (2024).
- <sup>27</sup>N. J. Douville *et al.*, “Combination of fluid and solid mechanical stresses contribute to cell death and detachment in a microfluidic alveolar model,” *Lab Chip* **11**, 609–619 (2011).
- <sup>28</sup>J. C. Mejías, M. R. Nelson, O. Liseth, and K. Roy, “A 96-well format microvascularized human lung-on-a-chip platform for microphysiological modeling of fibrotic diseases,” *Lab Chip* **20**, 3601–3611 (2020).
- <sup>29</sup>R. Plebani *et al.*, “Modeling pulmonary cystic fibrosis in a human lung airway-on-a-chip,” *J. Cystic Fibrosis* **21**, 606 (2022).
- <sup>30</sup>J. C. Nawroth *et al.*, “A microengineered airway lung chip models key features of viral-induced exacerbation of asthma,” *Am. J. Respir. Cell Mol. Biol.* **63**, 591–600 (2020).
- <sup>31</sup>H. Nazari, J. Shrestha, V. Y. Naei, S. R. Bazaz, M. Sabbagh, J. P. Thiery, and M. E. Warkiani, “Advances in TEER measurements of biological barriers in microphysiological systems,” *Biosens. Bioelectron.* **234**, 115355 (2023).
- <sup>32</sup>A. E. Ekpenyong, N. Toepfner, E. R. Chilvers, and J. Guck, “Mechanotransduction in neutrophil activation and deactivation,” *Biochim. Biophys. Acta BBA - Mol. Cell Res.* **1853**, 3105–3116 (2015).

- <sup>33</sup>M. S. Shive, M. L. Salloum, and J. M. Anderson, "Shear stress-induced apoptosis of adherent neutrophils: A mechanism for persistence of cardiovascular device infections," *Proc. Natl. Acad. Sci. U. S. A.* **97**, 6710–6715 (2000).
- <sup>34</sup>P. L. Candarlioglu *et al.*, "Organ-on-a-chip: Current gaps and future directions," *Biochem. Soc. Trans.* **50**, 665–673 (2022).
- <sup>35</sup>K. H. Benam *et al.*, "Small airway-on-a-chip enables analysis of human lung inflammation and drug responses *in vitro*," *Nat. Methods* **13**, 151–157 (2016).
- <sup>36</sup>L. Si *et al.*, "A human-airway-on-a-chip for the rapid identification of candidate antiviral therapeutics and prophylactics," *Nat. Biomed. Eng.* **5**, 815–829 (2021).
- <sup>37</sup>O. A. Forrest *et al.*, "Frontline science: Pathological conditioning of human neutrophils recruited to the airway milieu in cystic fibrosis," *J. Leukocyte Biol.* **104**, 665–675 (2018).
- <sup>38</sup>O. A. Forrest *et al.*, "Neutrophil-derived extracellular vesicles promote feed-forward inflammasome signaling in cystic fibrosis airways," *J. Leukocyte Biol.* **112**, 707–716 (2022).
- <sup>39</sup>S. L. Maas and E. P. C. van der Vorst, "In vitro (trans)migration experiment using chemokines as stimulatory factor," in *Chemokine-Glycosaminoglycan interactions: Methods and protocols*, edited by A. R. Lucas (Springer US, New York, 2023), pp. 77–87.
- <sup>40</sup>H. Viola *et al.*, "A high-throughput distal lung air–blood barrier model enabled by density-driven underside epithelium seeding," *Adv. Healthcare Mater.* **10**, 2100879 (2021).
- <sup>41</sup>M. Gschwandtner *et al.*, "Glycosaminoglycans are important mediators of neutrophilic inflammation *in vivo*," *Cytokine* **91**, 65–73 (2017).
- <sup>42</sup>A. Alfien *et al.*, "ADAMTS-13 regulates neutrophil recruitment in a mouse model of invasive pulmonary aspergillosis," *Sci. Rep.* **7**, 7184 (2017).
- <sup>43</sup>W. Adams, T. Espicha, and J. Estipona, "Getting your neutrophil: Neutrophil transepithelial migration in the lung," *Infect. Immun.* **89**, e00659 (2021).
- <sup>44</sup>W.-C. Lin and M. B. Fessler, "Regulatory mechanisms of neutrophil migration from the circulation to the airspace," *Cell. Mol. Life Sci.* **78**, 4095–4124 (2021).
- <sup>45</sup>R. Rubin, "Baricitinib is first approved COVID-19 immunomodulatory treatment," *JAMA* **327**, 2281 (2022).
- <sup>46</sup>V. Bronte *et al.*, "Baricitinib restrains the immune dysregulation in patients with severe COVID-19," *J. Clin. Invest.* **130**, 6409–6416 (2020).
- <sup>47</sup>A. M. Condliffe, E. R. Chilvers, C. Haslett, and I. Dransfield, "Priming differentially regulates neutrophil adhesion molecule expression/function," *Immunology* **89**, 105–111 (1996).
- <sup>48</sup>I. Miralda, S. M. Uriarte, and K. R. McLeish, "Multiple phenotypic changes define neutrophil priming," *Front. Cell. Infect. Microbiol.* **7**, 217 (2017).
- <sup>49</sup>I. Mazzitelli *et al.*, "Immunoglobulin G immune complexes may contribute to neutrophil activation in the course of severe coronavirus disease 2019," *J. Infect. Dis.* **224**, 575–585 (2021).
- <sup>50</sup>J.-C. Monboisse, R. Garnotel, A. Randoux, J. Dufer, and J.-P. Borel, "Adhesion of human neutrophils to and activation by type-I collagen involving a  $\beta 2$  integrin," *J. Leukocyte Biol.* **50**, 373–380 (1991).
- <sup>51</sup>M.-D. Filippi, "Neutrophil transendothelial migration: Updates and new perspectives," *Blood* **133**, 2149–2158 (2019).
- <sup>52</sup>M. R. Williams, V. Azcutia, G. Newton, P. Alcaide, and F. W. Luscinskas, "Emerging mechanisms of neutrophil recruitment across endothelium," *Trends Immunol.* **32**, 461–469 (2011).
- <sup>53</sup>Y. Gong *et al.*, "Dynamic contributions of P- and E-selectins to  $\beta 2$ -integrin-induced neutrophil transmigration," *FASEB J.* **31**, 212–223 (2017).
- <sup>54</sup>V. D. Gialalone, C. Margaroli, M. A. Mall, and R. Tirouvanziam, "Neutrophil adaptations upon recruitment to the lung: New concepts and implications for homeostasis and disease," *Int. J. Mol. Sci.* **21**, 851 (2020).
- <sup>55</sup>M. Mansoury, M. Hamed, R. Karmustaji, F. Al Hannan, and S. T. Safrany, "The edge effect: A global problem. The trouble with culturing cells in 96-well plates," *Biochem. Biophys. Res. Commun.* **26**, 100987 (2021).
- <sup>56</sup>G. A. Wilson *et al.*, "Human-specific epigenetic variation in the immunological leukotriene B4 receptor (LTB4R/BLT1) implicated in common inflammatory diseases," *Genome Med.* **6**, 19 (2014).
- <sup>57</sup>A. Ivetic, "Signals regulating L-selectin-dependent leucocyte adhesion and transmigration," *Int. J. Biochem. Cell Biol.* **45**, 550–555 (2013).
- <sup>58</sup>A. Ivetic, H. L. Hoskins Green, and S. J. Hart, "L-selectin: A major regulator of leukocyte adhesion, migration and signaling," *Front. Immunol.* **10**, 1068 (2019).
- <sup>59</sup>P. J. Middelhoven, A. Ager, D. Roos, and A. J. Verhoeven, "Involvement of a metalloprotease in the shedding of human neutrophil Fc $\gamma$ RIIIB," *FEBS Lett.* **414**, 14–18 (1997).
- <sup>60</sup>P. J. Middelhoven, J. D. van Buul, M. Kleijer, D. Roos, and P. L. Hordijk, "Actin polymerization induces shedding of Fc $\gamma$ RIIIB (CD16) from human neutrophils," *Biochem. Biophys. Res. Commun.* **255**, 568–574 (1999).
- <sup>61</sup>M. F. Tosi and H. Zakem, "Surface expression of Fc gamma receptor III (CD16) on 710 chemoattractant-stimulated neutrophils is determined by both surface shedding and 711 translocation from intracellular storage compartments," *J. Clin. Invest.* **90**(2), 462–470 (1992).
- <sup>62</sup>D. A. Moulding, C. A. Hart, and S. W. Edwards, "Regulation of neutrophil Fc $\gamma$ RIIIB (CD16) surface expression following delayed apoptosis in response to GM-CSF and sodium butyrate," *J. Leukocyte Biol.* **65**, 875–882 (1999).
- <sup>63</sup>E. Fortunati, K. M. Kazemier, J. C. Grutters, L. Koenderman, and V. J. M. M. Van den Bosch, "Human neutrophils switch to an activated phenotype after homing to the lung irrespective of inflammatory disease," *Clin. Exp. Immunol.* **155**, 559–566 (2009).
- <sup>64</sup>K. Ley, "Integration of inflammatory signals by rolling neutrophils," *Immunol. Rev.* **186**, 8–18 (2002).
- <sup>65</sup>S. C. J. Jorgensen, C. L. Y. Tse, L. Burry, and L. D. Dresser, "Baricitinib: A review of pharmacology, safety, and emerging clinical experience in COVID-19," *Pharmacotherapy* **40**, 843–856 (2020).
- <sup>66</sup>D. McGonagle, K. Sharif, A. O'Regan, and C. Bridgewood, "The role of cytokines including interleukin-6 in COVID-19 induced pneumonia and macrophage activation syndrome-like disease," *Autoimmun. Rev.* **19**, 102537 (2020).
- <sup>67</sup>G. U. Meduri *et al.*, "Inflammatory cytokines in the BAL of patients with ARDS: Persistent elevation over time predicts poor outcome," *Chest* **108**, 1303–1314 (1995).
- <sup>68</sup>N. Mukaida, "Pathophysiological roles of interleukin-8/CXCL8 in pulmonary diseases," *Am. J. Physiol.-Lung Cell. Mol. Physiol.* **284**, L566–L577 (2003).
- <sup>69</sup>S. Kubo *et al.*, "Janus kinase inhibitor baricitinib modulates human innate and adaptive immune system," *Front. Immunol.* **9**, 1510 (2018).
- <sup>70</sup>A. Ronit *et al.*, "Compartmental immunophenotyping in COVID-19 ARDS: A case series," *J. Allergy Clin. Immunol.* **147**, 81–91 (2021).
- <sup>71</sup>W. Huang *et al.*, "The inflammatory factors associated with disease severity to predict COVID-19 progression," *J. Immunol.* **206**, 1597–1608 (2021).
- <sup>72</sup>T. N. Hoang *et al.*, "Baricitinib treatment resolves lower-airway macrophage inflammation and neutrophil recruitment in SARS-CoV-2-infected rhesus macaques," *Cell* **184**, 460–475 (2021).
- <sup>73</sup>K. M. Henkels, K. Frondorf, M. E. Gonzalez-Mejia, A. L. Doseff, and J. Gomez-Cambronero, "IL-8-induced neutrophil chemotaxis is mediated by Janus kinase 3 (JAK3)," *FEBS Lett.* **585**, 159–166 (2011).
- <sup>74</sup>Z. Wang and E. C. Y. Chan, "Physiologically-based pharmacokinetic modelling to investigate baricitinib and tofacitinib dosing recommendations for COVID-19 in geriatrics," *Clin. Pharmacol. Ther.* **112**, 291–296 (2022).
- <sup>75</sup>J. Pillay *et al.*, "A subset of neutrophils in human systemic inflammation inhibits T cell responses through Mac-1," *J. Clin. Invest.* **122**, 327–336 (2012).
- <sup>76</sup>T. Tak *et al.*, "Human CD62Ldim neutrophils identified as a separate subset by proteome profiling and in vivo pulse-chase labeling," *Blood* **129**, 3476–3485 (2017).
- <sup>77</sup>R. Spijkerman *et al.*, "An increase in CD62Ldim neutrophils precedes the development of pulmonary embolisms in COVID-19 patients," *Scand. J. Immunol.* **93**, e13023 (2021).
- <sup>78</sup>R. Formiga and O. de *et al.*, "Cytosolic PCNA interacts with S100A8 controls an inflammatory subset neutrophils COVID-19," medRxiv (2022).
- <sup>79</sup>V. De Rose *et al.*, "Circulating adhesion molecules in cystic fibrosis," *Am. J. Respir. Crit. Care Med.* **157**, 1234–1239 (1998).
- <sup>80</sup>M. Declercq, L. Treps, P. Carmeliet, and P. Witters, "The role of endothelial cells in cystic fibrosis," *J. Cystic Fibrosis* **18**, 752–761 (2019).
- <sup>81</sup>R. Tirouvanziam, I. Khazaal, and B. Péault, "Primary inflammation in human cystic fibrosis small airways," *Am. J. Physiol.-Lung Cell. Mol. Physiol.* **283**, L445–L451 (2002).
- <sup>82</sup>C. Martin *et al.*, "Specific circulating neutrophils subsets are present in clinically stable adults with cystic fibrosis and are further modulated by pulmonary exacerbations," *Front. Immunol.* **13**, 1012310 (2022).
- <sup>83</sup>V. M. Kamp *et al.*, "Human suppressive neutrophils CD16bright/CD62Ldim exhibit decreased adhesion," *J. Leukocyte Biol.* **92**, 1011–1020 (2012).

<sup>84</sup>E. Oshika *et al.*, “Glucocorticoid-induced effects on pattern formation and epithelial cell differentiation in early embryonic rat lungs,” *Pediatr. Res.* **43**, 305–314 (1998).

<sup>85</sup>S. Hao, M. Andersen, and H. Yu, “Detection of immune suppressive neutrophils in peripheral blood samples of cancer patients,” *Am. J. Blood Res.* **3**, 239–245 (2013).

<sup>86</sup>M. Hassani *et al.*, “On the origin of low-density neutrophils,” *J. Leukocyte Biol.* **107**, 809–818 (2020).

<sup>87</sup>B. Dobosh, V. D. Giacalone, C. Margaroli, and R. Tirouvanziam, “Mass production of human airway-like neutrophils via transmigration in an organotypic model of human airways,” *STAR Protoc.* **2**, 100892 (2021).